Rare Metal Materials and Engineering
Volume 54, Issue 9, September 2025
Available online at www.rmme.ac.cn

Science Press

Cite this article as: Xing Quanyi, Zhou Ge, Zhang Haoyu, et al. Effect of Modification and Aging Treatments on Microstructure, Mechanical Properties and Electrical Conductivity of Al8Si0.4Mg0.4Fe Alloy[J]. Rare Metal Materials and Engineering, 2025, 54(09): 2247-2255. DOI: https://doi.org/10.12442/j.issn.1002-185X.20240455.

ARTICLE

Effect of Modification and Aging Treatments on Microstructure, Mechanical Properties and Electrical Conductivity of Al8Si0.4Mg0.4Fe Alloy

Xing Quanyi[1,2], Zhou Ge[1,2], Zhang Haoyu[1,2], Che Xin[1,2], Wang Wenjingzi[1,2], Chen Lijia[1,2]

[1] School of Materials Science and Engineering, Shenyang University of Technology, Shenyang 110870, China; [2] Shenyang Key Laboratory of Advanced Structural Materials and Applications, Shenyang University of Technology, Shenyang 110870, China

Abstract: Self-designed Al8Si0.4Mg0.4Fe aluminium alloy was modified with Sr, followed by solid solution and aging treatments to regulate its microstructure and mechanical/electrical properties. The results show that after the modification treatment, the room-temperature tensile strength of the alloy remains nearly unchanged, the elongation at break slightly increases from 1.82% to 3.34%, and the electrical conductivity significantly increases from 40.1% international annealed copper standard (IACS) to 42.0% IACS. After the modification, the alloy was subjected to solid solution treatment at 515 ℃ for 8 h, followed by aging treatment at 180, 200, 220 and 240 ℃ for 6 h. With increasing aging temperature, the electrical conductivity increases monotonously from 41.4% IACS to 45.5% IACS, while the room-temperature tensile strength initially increases and then decreases. At 200 ℃, the alloy achieves an optimal balance between electrical conductivity and room-temperature tensile strength: the electrical conductivity is 42.5% IACS, and the room-temperature tensile strength is 282.9 MPa. When the aging temperature continues to rise, the alloy undergoes overaging. Although the conductivity continues to increase, the room-temperature tensile strength drops sharply, and it is only 177.1 MPa at 240 ℃.

Key words: Al8Si0.4Mg0.4Fe alloy; electrical conductivity; aging treatment; room-temperature mechanical properties; microstructural evolution

1 Introduction

Aluminium alloys are widely used in automotive manufacturing, construction, electronics, aerospace, power systems and other fields, attributed to their low density, high specific strength, good corrosion resistance and excellent electrical/thermal conductivity[1–3]. In particular, the electric power industry has emerged as a critical pillar of China's infrastructure development. In recent years, driven by the global calls for energy savings and emission reduction, the traditional power generation has shifted from thermal to renewable sources such as wind, hydro, and solar sources[4]. To better cooperate with the energy-saving and environmental protection transition of power systems, according to the international low-carbon initiatives, reducing the power transmission losses has become an important direction, complementing the shift in power generation method. Therefore, the development of new power transmission conductors requires aluminium alloys to exhibit stable and reliable comprehensive mechanical properties while improving electrical conductivity. This is important for meeting the low-energy-consumption requirements of new long-distance overhead conductors and large load-bearing components in power transmission systems, such as conductive parts of transmission switches and transmission components.

Cast aluminium-silicon (Al-Si) alloys are widely utilized in structural parts with complex shapes for power transmission systems, attributed to their good castability, weldability, and low manufacturing costs[5]. Moreover, Al-Si alloys exhibit a low coefficient of linear expansion, making them preferable

Received date: August 25, 2024
Foundation item: Applied Basic Research Program of Liaoning Province (CN) (2022JH2/101300078)
Corresponding author: Zhou Ge, Ph. D., Professor, School of Materials Science and Engineering, Shenyang University of Technology, Shenyang 110870, P. R. China, E-mail: zhouge@sut.edu.cn

for parts requiring high dimensional accuracy across different temperature ranges[6–8]. The Si phase, serving as the primary strengthening phase in Al-Si alloys, plays a critical role in alloy design.

First, the Si content is a key factor influencing the strength of Al-Si alloys: the strength increases with increasing the Si content, yet Si increases electron scattering during transport, which results in a decrease in the plasticity and electrical conductivity of this alloy[9–11]. To solve the above problem, researchers have adopted microalloying design by introducing elements such as Mg, Cu, Ni and Fe to regulate the electrical conductivity and room-temperature strength of Al-Si alloys. Studies show that Mg can form Mg_2Si strengthening phase in the Al-Si alloy matrix, and the formation of minor second phase initially increases the thermal conductivity of the alloy[12], but beyond a threshold, increasing Mg content causes thermal conductivity to gradually decline[13–14]. Small amounts of Fe will form a Chinese character-like α-AlFeSi phase or needle-like β-AlFeSi phase in the matrix. These phases exhibit metallic characteristics, and their uniform distribution in the matrix promotes electrical conductivity. However, Ma et al[15] found that when the Fe content in Al-Si alloys is greater than 0.5%, the mechanical properties of the alloys decline sharply; however, with increasing the Mg content, the thermal conductivity begins to gradually decrease. The mechanical properties of the alloys decrease sharply. Therefore, the effect of alloying elements on electrical conductivity stems from the formation of second phases with different electrical conductivity coefficients, and conductivity decreases as the proportion of low-conductivity phases increases[16]. To balance strength and electrical conductivity optimally, scholars have attempted to further improve the comprehensive properties of Al-Si alloys through a combination of modification and heat treatment.

First, by adding Sr, Ni, Ce, Bi, Er and other modifying elements, eutectic Si is modified to form imperfect octahedral structures with primary dendrites or secondary dendrites after the modification treatment, which can significantly improve the strength and ductility of the alloys[17–19]. Second, heat treatments are used to reduce defects in as-cast alloys and to regulate their microstructure effectively. Specifically, solid solution strengthening and second-phase strengthening are the main mechanisms for enhancing the strength of alloys during heat treatments, while nanoscale precipitates formed during artificial aging can significantly increase the electrical conductivity of alloys[20–21]. However, Al-Si alloys generally exhibit a trade-off between electrical conductivity and strength, where conductivity decreases as strength increases. This inverse relationship between strength and electrical conductivity is currently a focus of academic research. Therefore, it is of particular importance for Al-Si alloys to improve the electrical conductivity of the alloy as the primary goal through the alloy system design, the selection of suitable modifiers, and implementation of corresponding solid solution+aging treatment. Based on them, good room-temperature mechanical properties can be ensured.

Therefore, this study investigated the effects of typical alloying elements (e. g., Cu, Fe and Mg) in Al-Si alloys, focusing on how their solid solubility and the resulting second phases influence alloy design. Notably, Fe has an extremely low solid solubility in Al, and without forming Fe-rich second phases, it has the least influence on the electrical conductivity of the alloy. However, due to its greater detrimental effect on mechanical properties, the content of Fe should be restricted to less than 0.5%[16]. In contrast, Cu and Mg have a large solid solubility in Al; their dissolution in the Al matrix induces lattice distortions, greatly enhancing electron scattering and thus reducing the electrical conductivity[22]. It is worth noting that although Mg has a maximum solid solubility of 18.6wt% in Al, its room-temperature solubility is only 1.2wt%. This allows the supersaturated Mg atoms to fully precipitate during artificial aging, forming Mg_2Si strengthening phases in conjunction with Si atoms, thus improving both strength and electrical conductivity. Based on the above considerations, this study independently designed an Al8Si0.4Mg0.4Fe alloy, ingeniously using Sr as a modifier to regulate the formation of fine fibrous eutectic Si with rounded tips. With this as-cast microstructure, a heat treatment of solid solution followed by aging was designed to explore the influence of the size and quantity of the second phase on the electrical conductivity and tensile strength of the alloy. The aim is to achieve an optimal balance between strength and electrical conductivity for this alloy, and to reveal the influence mechanism of modification and heat treatment processes on the microstructure, mechanical properties and electrical conductivity of the Al8Si0.4Mg0.4Fe alloy, providing solid theoretical support for expanding its practical applications.

2 Experiment

The experimental material was a self-designed AlSiMgFe alloy. Based on the designed mass ratio, the raw material included industrial-pure aluminium (99.7%), pure silicon (99.9%), industrial-pure magnesium (99.9%), pure iron (99.9%), and an Al-10Sr intermediate alloy. According to the designed alloy composition of the ingredients, the materials were melted using a well-type furnace. First, pure aluminium was melted at 750 ℃, followed by the addition of pure silicon and pure iron to the molten aluminium. After complete melting, pure Mg wrapped in aluminium foil was pressed to the bottom of the solution using a bell jar and gently stirred for 10 min. Subsequently, a hexachloroethane refining agent was added, the mixture was gently stirred, the slag was skimmed off, and the melt was left to stand for 10 min. The molten metal was then poured into the moulds, which were preheated at 200 ℃ to obtain aluminium alloy ingots. For the modification treatment, the melting process was identical to the above, with the Al-10Sr intermediate alloy added before refining. The alloy composition (wt%) was analyzed using inductively coupled plasma optical emission spectrometry (ICP-OES), and the results are listed in Table 1.

The alloy was subjected to solid solution and aging treatment in a box-type resistance furnace with the following

Table 1 Chemical composition of AlSiMgFe alloys

Alloy	Mg	Fe	Si	Sr	Al
Unmodified	0.453	0.423	8.16	-	Bal.
Modified	0.412	0.398	8.26	0.033	Bal.

process parameters: solid solution at 515 ℃ for 8 h followed by water cooling; aging at temperatures of 180–240 ℃ (interval of 20 ℃) for 6 h with air cooling. Microstructures before and after modification were observed using an Axio Observer Zeiss inverted optical microscope (OM). The specimens to be tested were polished step by step with 600#, 800#, 1000#, 1500# and 2000# sandpapers, followed by rough polishing with diamond abrasive paste (2.5 μm) and fine polishing using alumina suspension (0.05 μm). Subsequently, the specimens were etched in 0.5% hydrofluoric acid solution for 10 s, immediately cleaned with anhydrous ethanol after corrosion, and air-dried. The specimens for room-temperature mechanical property test were wire-cut according to the dimensional specifications in Fig. 1. Tensile tests were carried out in an MTS Landmark 370.10 testing machine to obtain the room-temperature yield strength (YS), ultimate tensile strength (UTS) and elongation (EL) of the Al8Si0.4Mg0.4Fe alloy. Three specimens were tested under each condition, and the results were averaged. Electrical conductivity was measured using a PZ-60A eddy current electrical conductivity meter, with five points per specimen tested and averaged. After separately performing surface treatments on the specimens before and after the modification treatment, the phase composition was analyzed using an XRD-7000 X-ray diffractometer (XRD). The parameters for the XRD test were as follows: the target material was Cu, the working voltage was 40 kV, the scanning angle was 20°–90°, and the scanning speed was 4°/min. Backscattered electron imaging via a SU8020 scanning electron microscope (SEM) was used to observe the second phase composition, as well as the tensile fracture morphology.

3 Results and Discussion

3.1 Effect of modification treatment on microstructure

The microstructures of the as-cast Al-Si alloys before and after modification are shown in Fig. 2a and 2b, respectively.

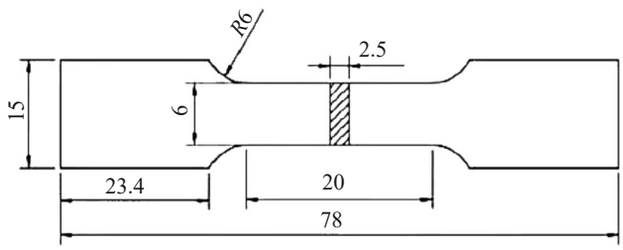

Fig.1 Dimensions of tensile specimen

An α-Al matrix and coarse lamellar eutectic silicon can be clearly observed in the unmodified alloy, and the lamellar eutectic silicon is randomly and haphazardly distributed in the matrix. After Sr modification, the eutectic silicon phase undergoes significant morphological changes: the plate-like structure evolves into small fibrous structures with rounded tip, while the α-Al phase in the microstructure exhibits an obvious rounded area, and its contact interface with the silicon phase becomes smooth and flat. This is due to the low solubility of Sr in Al: during the solidification process, Sr will be free at the liquid-solid interface front. When the eutectic temperature is reached, the eutectic Al-Si begins to grow in the interdendritic regions of α-Al dendrites. Concurrently, the Sr atoms that are free in the liquid phase are enriched at the growth front, inhibiting the growth rate of eutectic Si. Additionally, Sr adsorption on the growth steps of Si changes the growth direction of eutectic Si, leading to the formation of fibrous structures, which is consistent with the findings of Jenkinson et al[23]. To characterize phase composition changes after modification, XRD analysis was carried out on both unmodified and modified alloy (Fig. 2c). The results show that no new phases are generated in the modified alloy, and the as-cast microstructure mainly consists of the α-Al matrix, eutectic Si phase and a small number of AlFeSi and Mg_2Si phases.

Fig. 3a shows SEM image of the modified AlSiMgFe alloy, revealing three main reinforcing phases in the microstructure. In addition to the distinguished eutectic silicon phase, the other two phases were analyzed by energy-dispersive spectroscopy (EDS) at points A and B in Fig. 3a. The elemental composition of point A is Al, Fe and Si, which can be identified as the β-AlFeSi phase by combining with its long

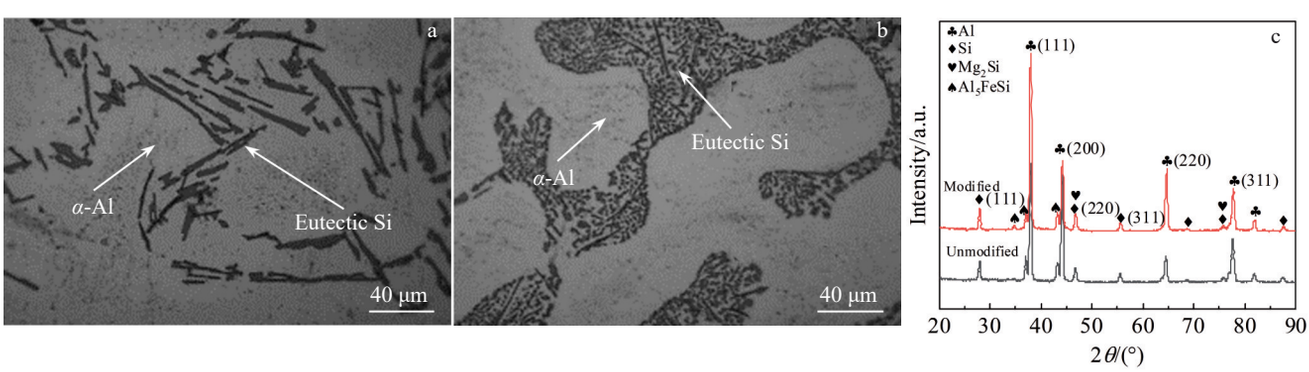

Fig.2 Microstructures (a–b) and XRD patterns (c) of the alloy before and after modification: (a) unmodified and (b) modified

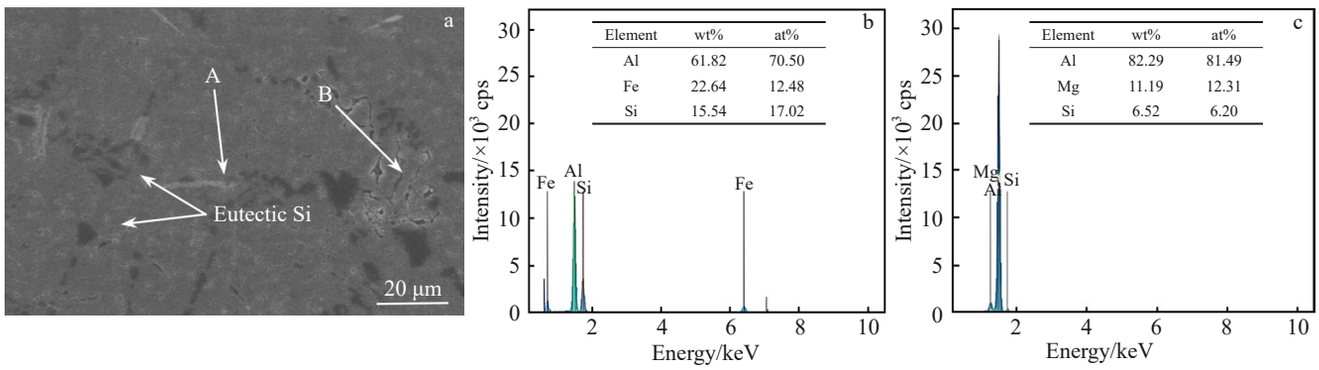

Fig.3 SEM image of the modified alloy (a) and EDS results of point A (b) and point B (c)

needle-like morphology. The EDS analysis of point B shows the presence of Al, Mg and Si at this point, with an atomic ratio of Mg to Si approaching 2:1. Based on the XRD analysis results, the black secondary phases exhibiting clustered distributions are identified as Mg_2Si phases. The maximum solubility of Mg in Al is 18.6%, but at room temperature, it drops to only 1.2%. When the Mg content exceeds the solid solubility, it precipitates from the Al matrix and combines with Si atoms to form Mg_2Si phase. In contrast, the solubility of Fe in Al is extremely low, and thus during solidification, nearly all the Fe atoms in the alloy composition remain undissolved. Instead, they exist in the matrix as iron-rich secondary phases, exhibiting not only the long needle-like morphology at point A in Fig. 3a but also Chinese character-like morphology in the Al-Si alloy. However, due to its low stability, such phases were not detected in the microstructure of this alloy.

3.2 Effect of modification treatment on electrical conductivity

Fig. 4 shows the schematics of electron movement in monatomic and polyatomic systems. After the modification treatment, the electrical conductivity of the as-cast Al-Si alloy increases from 40.1% international annealed copper standard (IACS) to 42.0% IACS. This improvement arises from the morphological transformation of eutectic silicon, which reduces obstruction to electron transport, and diminishes free electron scattering in the alloy matrix. In the monoatomic system, the electrons transition from lower to higher energy levels when they gain energy, thus leaving holes in their original positions, as shown in Fig.4a. In polyatomic systems, electrons can undergo tunneling transitions between adjacent atoms upon gaining energy[24]. Subsequent electrons will also undergo similar transitions to occupy the positions previously held by those electrons, thereby initiating the conduction of electrons in the conductor, as depicted in Fig.4b and 4c. As a semiconductor, Si has a relatively strong electron binding energy, requiring higher energy for electron transitions. The lack of vacancies in their lower energy levels hinders other electrons from entering, making the electrical conductivity of the Si phase significantly lower than that of metals. Fig. 5 shows electron transport mechanism in the Al-Si alloy, where the Si phase acts as the main obstacle to the electron transport, and the free electrons in Al preferentially move around the Si phase. According to classical electron theory, the resistivity of a conductor is directly proportional to electron scattering coefficient and inversely proportional to electron mean free path. After the modification treatment, the contact area between the eutectic Si phase and α-Al increases, which also enlarges gaps between eutectic Si particles, leading to an increase in the electron mean free path. As a result, the electrical conductivity of the Al-Si alloy is enhanced.

3.3 Effect of modification treatment on mechanical properties

Fig.6 shows the tensile test results of the Al-Si alloy before and after modification. The UTS of the alloy remains nearly unchanged after the modification, but EL at break significantly increases from 1.82% to 3.34%. In this alloy, the eutectic silicon phase, as the main reinforcing phase, dominates in both quantity and size, thus affecting the strength and plasticity of the alloy. The modification treatment changes

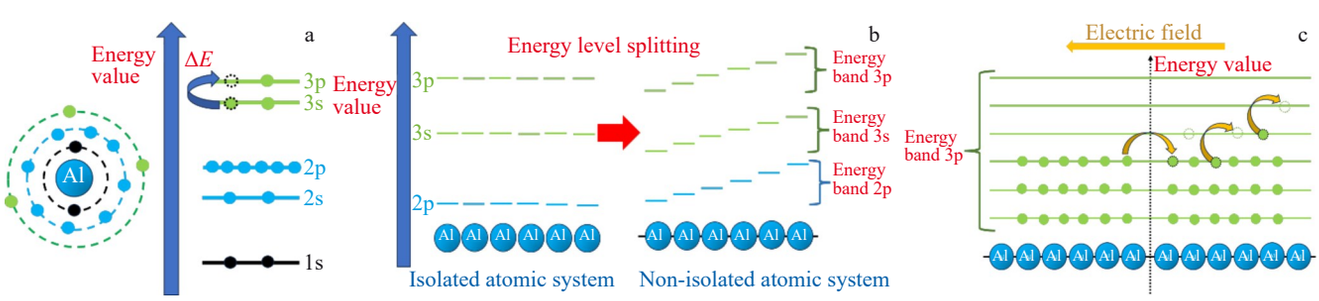

Fig.4 Schematics of electron movement: (a) monatomic system, (b) energy level splitting in polyatomic system, and (c) polyatomic system

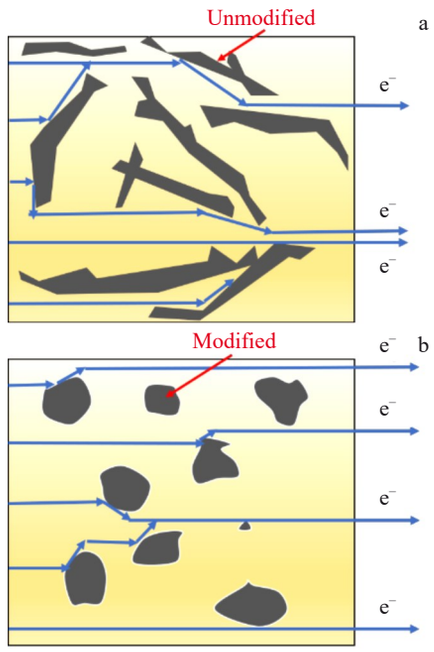

Fig.5 Schematics of electron transport before (a) and after (b) modification

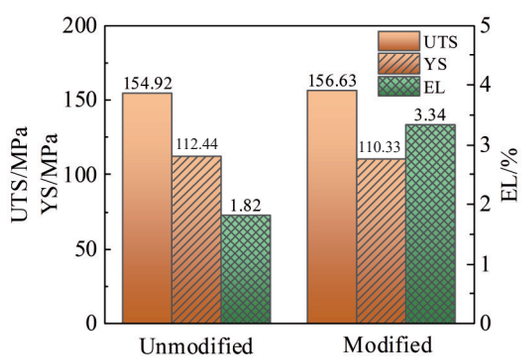

Fig.6 Mechanical properties of alloys before and after modification

the growth mode of eutectic silicon: the morphological transformation and size refinement reduce the fragmentation effect on the matrix, leading to a significant increase in the EL at break. After the addition of Sr modifier, the crystallization range of the alloy increases due to the inhibition of Si growth by the Sr, and the incipient α-Al grows into coarse dendrite structures, as shown in Fig.2b, which in turn induces a certain change in the fracture mode of the alloy. As seen from the tensile fracture morphologies before and after the modification treatment (Fig.7), the fracture morphology of the as-cast Al-Si alloy without modification treatment shows numerous cleavage planes, which is typical brittle fracture characteristic. Whereas the modified alloy displays quasi-cleavage features with sparse dimples near cleavage planes. The sufficient growth of the α-Al matrix and refinement of eutectic silicon contribute to the slight reduction in both UTS and YS.

Therefore, after the Sr modification treatment, the morphology of the eutectic silicon in the alloy microstructure effectively changes, resulting in increased electrical

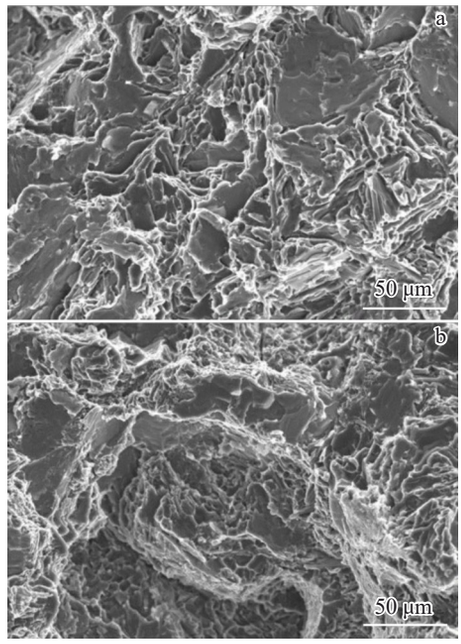

Fig.7 Tensile fracture morphologies of unmodified (a) and modified (b) alloys

conductivity and EL at break of the alloy. However, the modification has a negligible impact on other strengthening phases, resulting in relatively low UTS. During alloy solidification, supersaturated Mg atoms dissolved in the α-Al matrix cannot be precipitated via modification treatment. Therefore, the solid solution followed by aging is used to further purify the matrix, reduce the lattice distortion of the α-Al matrix, and promote the sufficient and uniform precipitation of solute atoms. This process forms a dispersive second phase, enabling additional strengthening of the alloy.

3.4 Effect of aging temperature on microstructure

Fig.8 shows the microstructures of the alloys after aging at different temperatures. After the solid solution and aging treatment, the eutectic silicon phase in the modified alloy undergoes obvious spheroidization, and large eutectic silicon phases fuse during the heat treatment and split into finer particles, which decreases the average size of the eutectic silicon phase and increases the number of particles. The size and morphology of the β-AlFeSi phase remain unchanged, continuing to exhibit randomly distributed long needle-like structures within the matrix.

As the aging treatment temperature increases, the Mg_2Si phase in the alloy gradually increases in both quantity and size, as shown in Fig.8. At an aging temperature of 180 ℃, no Mg_2Si precipitates are observed in the Al-Si alloy microstructure, which indicates that at this temperature, all Mg remains dissolved in the matrix after solid solution treatment, and 180 ℃ is insufficient to induce Mg precipitation. When the aging temperature increases to 200 ℃, very fine Mg_2Si particles are observed in the matrix and dispersed in the matrix. Further increasing the aging temperature promotes continuous growth of Mg_2Si: the size reaches approximately

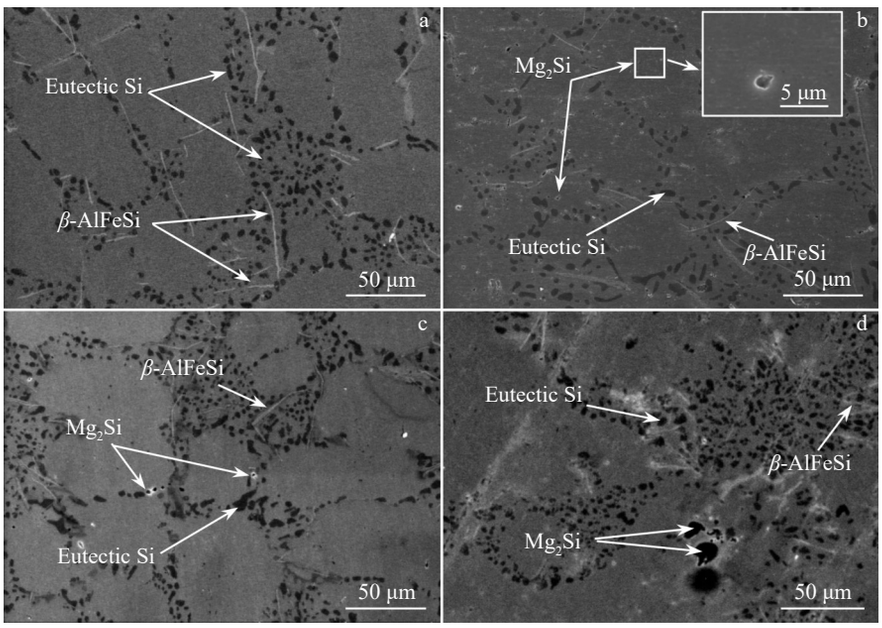

Fig.8 SEM images of the alloy at different aging temperatures: (a) 180 ℃, (b) 200 ℃, (c) 220 ℃, and (d) 240 ℃

3 μm at 220 ℃, accompanied by the onset of overaging. At 240 ℃, the particles grow to 10 μm in size.

During the aging process, in addition to changes in the morphology and quantity of major second phases in the alloy microstructure, fine nanoscale precipitates form inside these second phases, which will have a positive impact on the electrical conductivity and mechanical properties of the alloy[25]. As shown in Fig. 9a, these fine nanoscale precipitates are distributed abundantly at the interface between the matrix and the second phase as spherical particles. To determine the composition of these phases, EDS analysis was performed on points A, B and C in Fig. 9a, and the results are shown in Fig. 9b – 9d. Point A corresponds to the Al matrix, and the second phase that serves as the carrier of nanoscale precipitates is the eutectic Si phase. These fine nanoscale precipitates contain Al and Si elements. Since eutectic silicon serves as the substrate of these black particles and its size is too small, Si contamination is inevitable during the analysis. Therefore, it can be inferred that these nanoscale precipitates are spherical Al particles, consistent with the research results of Xi et al[26]. The presence of these nanoscale Al particles increases the local free electron density and reduces the

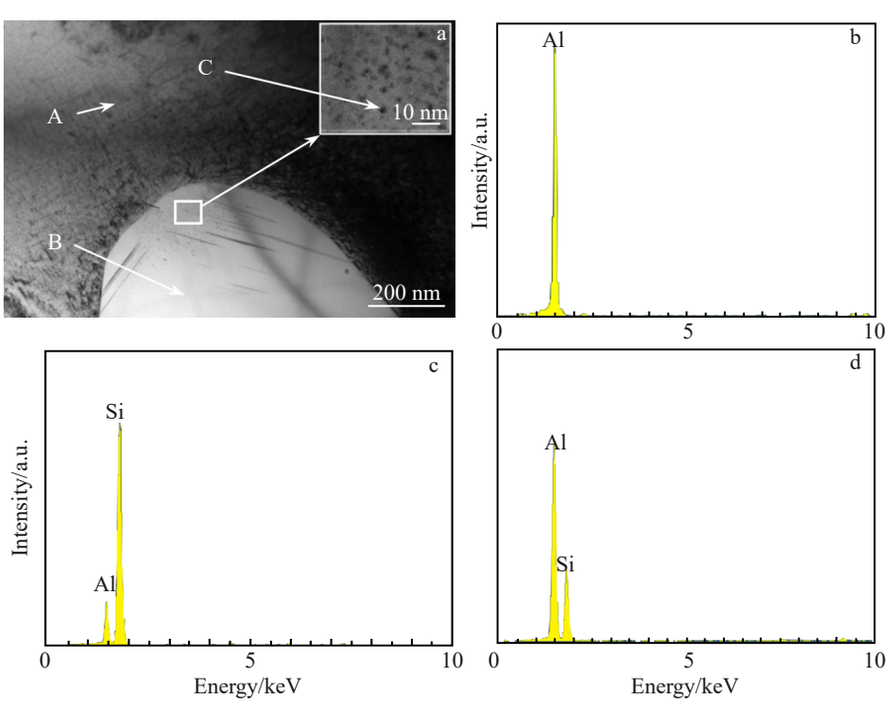

Fig.9 TEM images of nanoscale precipitates (a) and corresponding EDS spectra (b–d): (b) point A, (c) point B, and (d) point C

fracture tendency of the Si phase, thus promoting the improvement of electrical conductivity and strength.

3.5 Effect of aging temperature on electrical conductivity

Fig. 10 shows the electrical conductivity of the alloy at different aging temperatures. As the aging temperature increases, the electrical conductivity of the alloy increases and eventually plateaus out. At 180 ℃, all Mg atoms and a minor number of Si atoms are dissolved in the α-Al matrix, which reduces the purity of the Al matrix and decreases the free electron density in the matrix. The increased defect density in the Al matrix exacerbates the lattice distortion in the crystals, shortening the mean free path of electrons, and decreasing the electrical conductivity of the alloy. At 200 ℃, Mg begins to precipitate in the Al matrix and combines with Si atoms to form the Mg_2Si phase due to the strong binding ability of Mg and Si. Although both Mg_2Si and Si are semiconductors, the electrical conductivity of Mg_2Si is much higher than that of Si[23], and the precipitated Mg atoms consume portions of the electrical conductivity during the formation of the second phase of Mg_2Si in the microstructure. The eutectic Si phase with poorer electrical conductivity is consumed by the precipitated Mg atoms, and the α-Al matrix is purified, resulting in an increase in the electrical conductivity of the alloy. With further temperature elevation, the alloy undergoes overaging. The Mg_2Si phases precipitated in the alloy microstructure coarsen. Since Al matrix maintains the primary channel for electron transport, the growth of this second phase minimally obstructs this pathway, and the number of primary channels in the electron transport process does not change much, i. e., the electrical conductivity of the alloy changes negligibly at temperatures higher than 220 ℃.

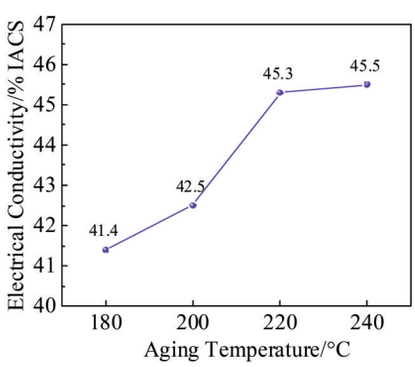

Fig.10 Electrical conductivity of alloys at different aging temperatures

The eutectic Si phase becomes more rounded after heat treatment, and the large Si phase undergoes disintegration to form fine Si particles. The increased interstitial space between the Si particles expands electron transport channels, resulting in a slight increase in electrical conductivity.

After solid solution treatment and aging at different temperatures, the morphology, size and quantity of Fe-rich phase show negligible changes. The solubility of Fe in Al is very low or even negligible, so the Fe in this alloy exists as Fe-rich second phase in the alloy microstructure, predominantly as β-AlFeSi phase with trace amounts of α-AlFeSi phase. Due to the low content of α-AlFeSi, it is not observed in this alloy microstructure. The β -AlFeSi phase exhibits metallic characteristics and has a small effect on the electrical conductivity[27]. Fe consumes some of the Si atoms with poor electrical conductivity in the alloy, reducing the amount of Si phase, which has a certain promotion effect on the electrical conductivity of the alloy. This promoting effect is equivalent at different aging temperatures, and the change in the electrical conductivity of the alloy is mainly due to the number and size of the Mg_2Si phase and the purity of the α-Al matrix.

3.6 Effect of aging temperature on alloy strength

Fig. 11a shows the tensile stress-strain curves at different aging temperatures. The UTS of the alloy increases and then decreases with increasing temperature, reaching a maximum value of 282.9 MPa at 200 ℃ (Fig. 11b), at which the electrical conductivity is 42.5% IACS. At 180 ℃, Mg and minor Si atoms are dissolved in the matrix, the lattice distortion of the matrix increases, and the resistance of dislocation movement in the matrix increases, resulting in solid solution strengthening. At the same time, coarse eutectic Si particles are refined and spheroidized, with increased roundness and dispersion, contributing to dispersion strengthening. The simultaneous existence of these two main strengthening modes results in a substantial increase in the tensile strength of the alloy compared to that at the as-cast state. At an aging temperature of 200 ℃, the dissolved Mg

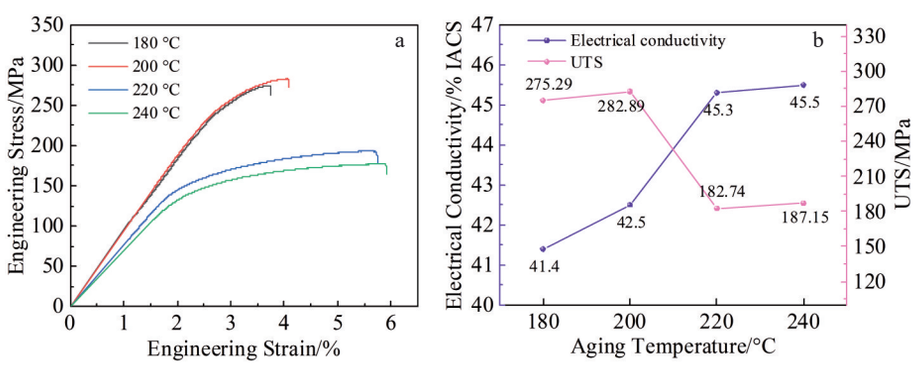

Fig.11 Tensile stress curves (a) and electrical conductivity and UTS (b) of specimens at different aging temperatures

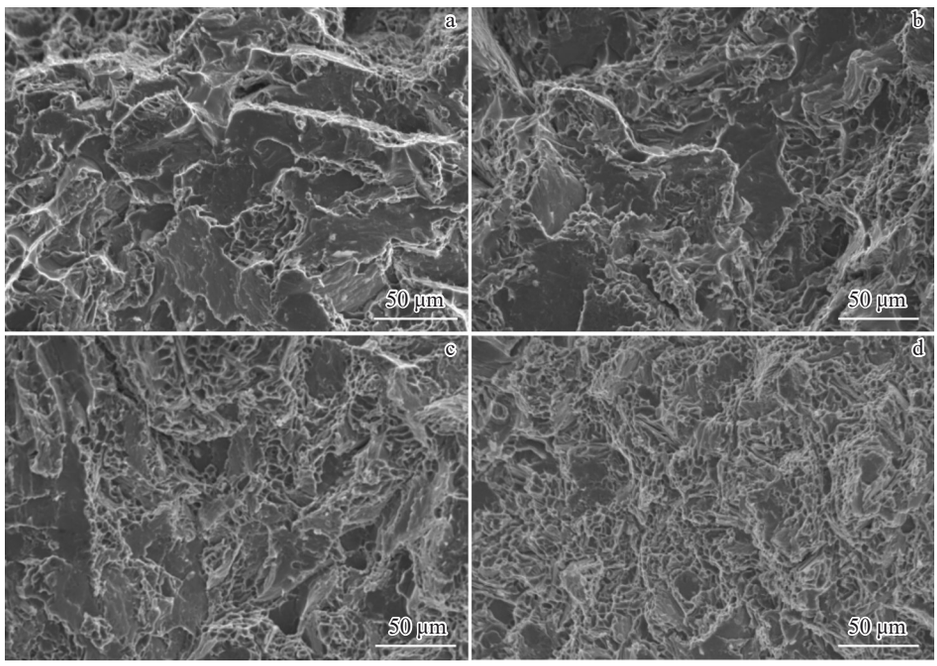

Fig.12 Tensile fracture morphologies at different aging temperatures: (a) 180 ℃, (b) 200 ℃, (c) 220 ℃, and (d) 240 ℃

and Si atoms precipitate to form a dispersed fine Mg_2Si phase, as shown in Fig.8b. Due to the small atomic radius difference between the Mg and Al, substitutional solid solution causes minimal lattice distortion, and the second-phase strengthening effect produced when the Mg atoms precipitate from the solid solution is much greater than solid solution strengthening, which leads to further increase in the tensile strength of the alloy. When the temperature continues to increase, the dispersed Mg_2Si phases are aggregated and coarsened, weakening dispersion strengthening. Moreover, the size of the eutectic Si phase increases, and the roundness begins to decrease, leading to strength degradation of the alloy. Fracture morphologies of the tensile specimens under different heat treatment conditions (Fig.12) show that with increasing aging temperature, the dimples in the fracture morphology of the tensile specimens gradually increase, and the cleavage effect on the matrix is weakened due to the tip passivation and spheroidization produced by the brittle eutectic Si phase, which gradually decreases the cleavage plane area of the alloy. When the aging temperature reaches 220 ℃, the Mg_2Si phases dispersed in the matrix are aggregated and grow, as shown in Fig. 8c – 8d, which reduces the resistance to dislocation movement in the α-Al matrix, enhancing the plasticity of the Al matrix and increasing dimple density in the tensile fracture surface, and thus resulting in a decrease in the strength but an increase in plasticity. Although the β-AlFeSi phase has a high hardness, it exists as long needles in the matrix, and it is not possible to change its morphology by heat treatment. This morphology produces a cleavage effect on the matrix, which is detrimental to the mechanical properties of Al-Si alloys. However, the β -AlFeSi phase exhibits metallic characteristics[28–29], and when it is uniformly distributed in an aluminium matrix, it has virtually no effect on the electrical conductivity of the alloy. Additionally, the presence of trace AlFeSi ternary phase reduces the content of the Si phase in the alloy, which leads to a slight increase in the electrical conductivity of Al-Si alloys.

4 Conclusions

1) After the Sr modification treatment of Al8Si0.4Mg0.4Fe alloy, the morphology transformation of eutectic Si phase in the microstructure reduces electron scattering, significantly enhancing the electrical conductivity of the alloy from 40.1% to 42.0% IACS. While the tensile strength shows no negligible improvement, the fibrous eutectic Si has a weaker fragmentation effect on the substrate compared to the plate-like eutectic Si, improving plasticity from 1.82% to 3.34%.

2) The modified alloy is subjected to solution treatment at 515 ℃ and aging treatment at 200 ℃ to achieve simultaneous increase in electrical conductivity and strength. During the aging process, Mg atoms dissolved in the α -Al matrix precipitate uniformly to form fine, dispersed Mg_2Si phases with Si atoms. The α-Al matrix is sufficiently purified, the electrical conductivity of the alloy increases to 42.5% IACS, and the dispersion strengthening effect from the Mg atoms in the second phase is much greater than solid solution strengthening in the matrix, enhancing resistance to dislocation motion. The tensile strength increases to 282.9 MPa.

3) Under the combined effect of modification and heat treatment, the morphology and quantity of eutectic Si and Mg_2Si phases in the alloy structure undergo significant changes. These changes in the second phase distinctly alter the electrical conductivity of the alloy, demonstrating that the Al8Si0.4Mg0.4Fe alloy can achieve concurrent enhancement of conductivity and strength through a combination of modification and heat treatment.

References

1 Sahoo B, Das T, Paul J *et al. Surface Review and Letters*[J], 2022, 29(9): 1

2 Sang Kyu Y, Ji Won K, Myung Hoon O *et al. Materials*[J], 2022, 15(17): 6103

3 Chen Weihao, Liu Fencheng, Niu Pengliang *et al. Rare Metal Materials and Engineering*[J], 2024, 53(4): 1111 (in Chinese)

4 Tayeb M, Frida G C, Jose R *et al. IEEE Power and Energy Magazine*[J], 2019, 17(3): 22

5 Esmeralda A, Arenas-García H, Rodríguez A *et al. Thermochimica Acta*[J], 2019, 675: 172

6 Callegari B, Lima N T, Coelho S R. *Metals*[J], 2023, 13(7): 1174

7 Haghayeghi R, Timelli G. *Materials Letters*[J], 2021, 283: 128779

8 Toshio H, Shinjiro I, Hiroshi F. *Materials*[J], 2021, 14(18): 5372

9 Chen J K, Hung H Y, Wang C F *et al. Journal of Materials Science*[J], 2015, 50: 5630

10 Wu L, He B, Li W D *et al. Journal of Physics: Conference Series*[J], 2021, 2133(1): 012021

11 Wang Y J, Liao H C, Wu Y N *et al. Materials & Design*[J], 2014, 53: 634

12 Li X H, Cui X L, Liu H Y *et al. Journal of Materials Science*[J], 2023, 58: 8478

13 Kimura T, Nakamoto T, Ozaki T *et al. Materials Science and Engineering A*[J], 2019, 754: 786

14 Guo W C, Chen X H, Liu P *et al. Advanced Engineering Materials*[J], 2021, 23(3): 2000955

15 Ma Z, Samuel A M, Doty H W *et al. Materials & Design*[J], 2014, 57: 366

16 Stadler F, Antrekowitsch H, Fragner W *et al. Materials Science and Engineering A*[J], 2013, 560: 481

17 Zhang J, Zhou Y P, Sun C C *et al. Materials Science Forum*[J], 2020, 993: 12

18 Li Y X, Fu Y T, Nie X *et al. Key Engineering Materials*[J], 2022, 921: 3

19 Fang W Q, Shen J R, Yan J K *et al*. *Rare Metal Materials and Engineering*[J], 2023, 52(7): 2326

20 Yu W B, Zhao H B, Wang L *et al. Journal of Alloys and Compounds*[J], 2018, 731: 444

21 Zhang Yunsheng, Jiang Xueyu, Zhou Ge *et al. Rare Metal Materials and Engineering*[J], 2024, 53(1): 38

22 Kim C W, Cho J I, Choi S W *et al. Advanced Materials Research*[J], 2013, 813: 175

23 Jenkinson D C, Hogan L M. *Journal of Crystal Growth*[J], 1975, 28(2): 171

24 Wei Dan. *Solid State Physics*[M]. Beijing: Tsinghua University, 2007 (in Chinese)

25 Hou J P, Wang Q, Zhang Z J *et al. Materials & Design*[J], 2017, 132: 148

26 Xi H H, Ming W Q, He Y *et al. Journal of Alloys and Compounds*[J], 2022, 906: 164238

27 Fang C M, Que Z P, Fan Z. *Journal of Solid State Chemistry*[J], 2021, 299: 122199

28 Allamki A, Al-Maharbi A, Qamar S Z *et al*. *Metals*[J], 2023, 13(6): 1111

29 Kim J M, Yun H S, Park J S *et al. International Journal of Cast Metals Research*[J], 2013, 27(3): 141

变质处理和时效处理对Al8Si0.4Mg0.4Fe合金组织、力学性能及电导率的影响

邢全义[1,2]，周　舸[1,2]，张浩宇[1,2]，车　欣[1,2]，王文静子[1,2]，陈立佳[1,2]

(1. 沈阳工业大学 材料科学与工程学院，辽宁 沈阳 110870)

(2. 沈阳工业大学 沈阳市先进结构材料与应用重点实验室，辽宁 沈阳 110870)

摘　要：对自主设计的Al8Si0.4Mg0.4Fe合金进行了Sr变质处理及固溶+时效处理，以调节其组织和性能。结果表明：变质处理后，合金的室温抗拉伸强度变化不大，断裂伸长率略有提高（1.82%至3.34%），电导率由变质处理前的40.1% IACS显著提高到42.0% IACS。将变质处理后的合金在515 ℃固溶处理8 h，然后在180、200、220和240 ℃时效处理6 h。随着时效温度的升高，材料的电导率由41.4% IACS单调增加到45.5% IACS，室温抗拉伸强度先升高后降低。在200 ℃时，合金的电导率与室温抗拉伸强度表现出良好的协调性，电导率为42.5% IACS，室温抗拉伸强度为282.9 MPa。当时效温度继续升高时，合金产生过时效现象。虽然电导率仍在上升，但室温抗拉伸强度急剧下降，在时效温度240 ℃时仅为177.1 MPa。

关键词：Al8Si0.4Mg0.4Fe合金；电导率；时效处理；室温力学性能；显微组织演变

作者简介：邢全义，男，1993年生，硕士，沈阳工业大学材料科学与工程学院，辽宁 沈阳 110870，E-mail：quanyi1022@163.com